Force Distributions near Jamming and Glass Transitions

Corey S. O'Hern,[1,3] Stephen A. Langer,[2] Andrea J. Liu,[1] and Sidney R. Nagel[3]
[1]*Department of Chemistry and Biochemistry, University of California at Los Angeles, Los Angeles, California 90095-1569*
[2]*Information Technology Laboratory, NIST, Gaithersburg, Maryland 20899-8910*
[3]*James Franck Institute, The University of Chicago, Chicago, Illinois 60637*
(Received 2 May 2000)

We calculate the distribution of interparticle normal forces $P(F)$ near the glass and jamming transitions in model supercooled liquids and foams, respectively. $P(F)$ develops a peak that appears near the glass or jamming transitions, whose height increases with decreasing temperature, decreasing shear stress and increasing packing density. A similar shape of $P(F)$ was observed in experiments on static granular packings. We propose that the appearance of this peak signals the development of a yield stress. The sensitivity of the peak to temperature, shear stress, and density lends credence to the recently proposed generalized jamming phase diagram.

DOI: 10.1103/PhysRevLett.86.111 PACS numbers: 64.70.Pf, 81.05.Rm, 83.70.Hq

Granular materials can flow when shaken, but jam when the shaking intensity is lowered [1]. Similarly, foams and emulsions can flow when sheared, but jam when shear stress is lowered [2]. These systems are athermal because thermal energy is insufficient to change the packing of grains, bubbles, or droplets. When the external driving force is too small to cause particle rearrangements, these materials become amorphous solids and develop a yield stress. A supercooled liquid, on the other hand, is a *thermal* system that turns, as temperature is lowered, into a glass—an amorphous solid with a yield stress [3]. Despite significant differences between driven, athermal systems and quiescent, thermal ones, it has been suggested that the process of jamming—developing a yield stress in an amorphous state—may lead to common behavior, and that these systems can be unified by a jamming phase diagram [4]. This implies that there should be similarities in these different systems as they approach jamming or glass transitions. We test this speculation by measuring the distribution $P(F)$ of interparticle normal forces F, in model supercooled liquids and foams. We find that for glasses, $P(F)$ is quantitatively similar to experimental results on granular materials [5].

When granular materials jam, the distribution of stresses is known to be inhomogeneous [6,7]. As proposed in Ref. [7], we quantify this effect by measuring $P(F)$. Our aim is to determine which feature in $P(F)$ is associated with development of a yield stress. Experiments [5,8] and simulations [9,10] on static granular packings find that $P(F)$ has a plateau or small peak at small F and decays exponentially at large F. We argue that the development of a peak is the signature of jamming.

For supercooled liquids, equilibrium statistical mechanics gives insight into the shape of $P(F)$. Since forces depend only on particle separations, $P(F)dF = G(r)dr$, where $G(r)dr$ is the probability of finding a particle between r and $r + dr$ given a particle at the origin. Thus, $G(r) = \rho/(N-1)S_D r^{D-1} g(r)$, where N is the number of particles, ρ is the number density, $g(r)$ is the pair distribution function, and $S_D r^{D-1}$ is the surface area of a D-dimensional sphere of radius r. Although it is well known that $g(r)$ does not change significantly as the temperature is varied through the glass transition T_g, we show below that $P(F)$ is quite sensitive and actually develops a peak near T_g. Physically, forces (or stresses [11,12]) are crucial for understanding the slowing down of stress relaxation near the glass transition, or the development of a yield stress. It is therefore not surprising that $P(F)$, which is a particular weighting of $g(r)$, is much more sensitive to the glass transition than $g(r)$ itself.

In a jammed system like a granular material, an analytic expression for $g(r)$ is not known and $P(F)$ must be measured directly. However, in an *equilibrium* system at temperature T, the large-force behavior of $P(F)$ can be obtained from the small-separation behavior of $g(r)$: $g(r) = y(r)\exp[-V(r)/k_b T]$, where $V(r)$ is the pair potential and $y(r)$ depends relatively weakly on r at small r [13]. This leads to

$$P[F(r)] \sim y(r) r^{D-1} \frac{dr}{dF} \exp[-V(r)/k_b T]. \qquad (1)$$

From our simulations, we compute the force distributions in systems that are out of equilibrium, such as glasses and sheared foams, as well as systems in equilibrium, such as supercooled liquids. We find that $P(F)$ for supercooled liquids (with sufficiently strong repulsive potentials) decays approximately exponentially at large forces, as predicted by Eq. (1). Because this is true at all temperatures, even those far above T_g, the exponential tail is not necessarily a signature of an amorphous solid.

We perform constant-temperature molecular dynamics simulations on binary mixtures in 2D, using the Gaussian constraint thermostat and leapfrog Verlet algorithm [14]. The masses m of the particles are the same, but the ratio of particle diameters, $\sigma_2/\sigma_1 = 1.4$, ensures that the system does not crystallize [12]. We confine $N = 1024$ particles

(512 of each variety) to a square box and use periodic boundary conditions. For each simulation, we choose one of the following interparticle pair potentials:

$$\begin{aligned}
V_{ab}^{\mathrm{SC}}(r) &\equiv \epsilon(\sigma_{ab}/r)^{12}, \\
V_{ab}^{\mathrm{LJ}}(r) &\equiv 4\epsilon[(\sigma_{ab}/r)^{12} - (\sigma_{ab}/r)^{6}], \\
V_{ab}^{\mathrm{LJR}12}(r) &\equiv 4\epsilon[(\sigma_{ab}/r)^{12} - (\sigma_{ab}/r)^{6}] + \epsilon; \\
r/\sigma_{ab} &\leq 2^{1/6}, \\
V_{ab}^{\mathrm{LJR}24}(r) &\equiv \frac{2^{8/3}\epsilon}{3}[(\sigma_{ab}/r)^{24} - (\sigma_{ab}/r)^{6}] + \epsilon; \\
r/\sigma_{ab} &\leq 2^{1/9},
\end{aligned} \tag{2}$$

where $\sigma_{ab} = (\sigma_a + \sigma_b)/2$ for $a, b = 1, 2$. The potentials LJR12 and LJR24 are zero above the specified cutoffs. (The potentials SC and LJ are truncated at large r, $r/\sigma_{ab} = 4.5$.) Below, we measure time, force, temperature, and density in units of $\sigma_1(m/\epsilon)^{1/2}$, ϵ/σ_1, ϵ/k_b, and σ_1^{-2}, respectively. The simulations on purely repulsive potentials SC, LJR12, and LJR24 simulations were carried out at constant density $\rho = 0.747$; the simulations on LJ, which include an attraction, were carried out at zero average pressure.

The hallmark of the glass transition is the extreme slowing down of the dynamics as temperature is lowered toward the glass transition. The pair potentials in Eq. (2) all give rise to glass transitions as temperature is lowered [12]. We determine T_g by measuring the self-part of the intermediate scattering function $F_2(k_p, t)$ for the large particles at a wave vector k_p corresponding to the first peak of the static structure factor [12,15]. For high temperatures, the liquid equilibrates quickly and $F_2(k_p, t)$ decays exponentially to zero. The relaxation time τ_r is defined as the time at which $F_2(k_p, t)$ decays to $1/e$; this is a measure of the α-relaxation time [12,15]. Since τ_r increases so rapidly near the glass transition, simulations can only reach equilibrium for temperatures $T > T_g$, where T_g is determined when τ_r exceeds a predetermined, large value, which we take to be $\tau_r > 1000$. For our parameter choices, the glass transition temperatures are $T_g^{\mathrm{SC}} = 0.38$, $T_g^{\mathrm{LJR}12} = 1.1$, $T_g^{\mathrm{LJR}24} = 3.0$, and $T_g^{\mathrm{LJ}} = 0.17$.

For $T > T_g$ we measure $P(F)$ for all interparticle force pairs from at least 250 configurations after equilibrating each configuration for $10-100\tau_r$. The top frame of Fig. 1 shows $P(F)$ plotted versus F/T for LJR12 for seven temperatures above T_g with temperature decreasing from top to bottom. At high temperatures, we see in the top frame of Fig. 1 that $P(F)$ increases with decreasing F over the entire range of F. However, as temperature is lowered towards T_g, a plateau in $P(F)$ forms at forces below the average $\langle F \rangle$. By shifting each curve vertically, we have obtained collapse of the high-force data for all of these *equilibrium* systems. From Eq. (1), we expect that the large-force tail should scale asymptotically as $\exp(-BF^{12/13}/T)$, where B is a constant and the power $12/13$ derives from the $1/r^{12}$ repulsion. Thus, for particles with harder cores (steeper repulsions), the tail becomes closer to an exponential in F, as seen in experiments on granular materials [5]. This explanation for the exponential tail is different from that of the q model [7] and its generalizations [16] based on stochastic force propagation. Previous LJ simulations along the liquid-vapor coexistence line [17] showed that the Cartesian components of the force also have an exponential distribution. Our results are related to theirs: for high forces, the total force on a particle, which is the vector sum of the normal forces, will be dominated by the largest normal force. This is why the distribution of Cartesian components is also exponential.

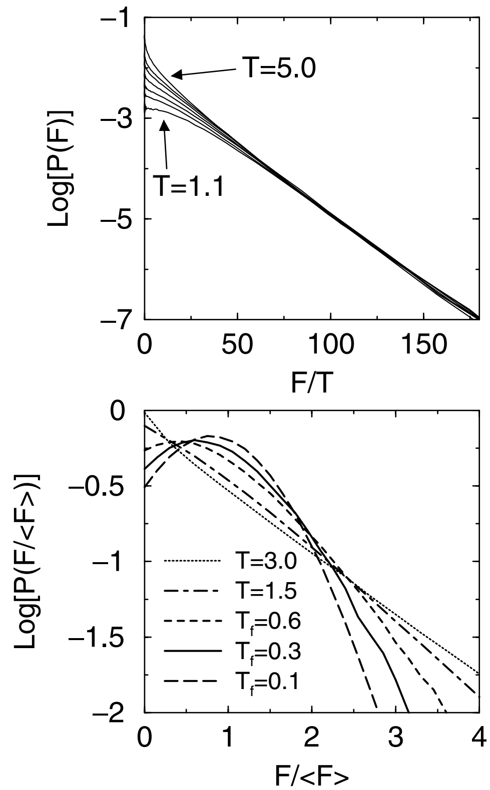

FIG. 1. Top: $P(F)$ for all interparticle force pairs versus F/T for LJR12 (a purely repulsive potential) obtained for seven temperatures above T_g with T decreasing from top to bottom. Bottom: $P(F/\langle F \rangle)$ versus $F/\langle F \rangle$ for LJR12 for two temperatures above and three below T_g.

We also study $P(F)$ *out* of equilibrium by performing thermal quenches from $T_i > T_g$ to T_f. The results discussed below are relatively insensitive to changes in T_i or quench rate, but depend on whether T_f lies above or below T_g. For $T_f > T_g$, $P(F)$ initially develops a region of lower (but still negative) slope at high forces, which moves to lower forces and disappears as the system equilibrates. In the bottom frame of Fig. 1, we show the long-time behavior of $P(F)$ for LJR12 following a quench below $T_g \approx 1.1$ to $T_f = 0.6$, 0.3, and 0.1. For comparison, two equilibrium distributions at $T = 1.5$

and 3.0 are also shown. We scaled the abscissa by $\langle F \rangle$ (which increases with T). There are two significant features in $P(F)$ for glasses. First, the slope of the exponential tail increases as T is lowered. The temperature corresponding to the tail T_{tail}, however, is not the final temperature T_f, but rather satisfies $T_f < T_{\mathrm{tail}} < T_g$. Thus, a fraction of the large thermal forces cannot relax in the glassy state. The second significant feature of $P(F)$ for glasses is the formation of a peak near $\langle F \rangle$, as shown in the bottom frame of Fig. 1. Thus, in contrast to $g(r)$, there is a significant change in $P(F)$ below T_g. The behavior of $P(F)$ for $F > 0$ when quenched below T_g is qualitatively the same for all potentials and densities studied, showing that the peak signals the glass transition in a system with attractive interactions and no applied pressure as well as systems with purely repulsive interactions under pressure.

The potentials LJR12 and LJR24 in Eq. (2) are most similar to granular materials since they produce purely repulsive forces that vanish at small separation. We compare $P(F/\langle F \rangle)$ in the glassy state for LJR12 and LJR24 to $P(F/\langle F \rangle)$ for static granular packings in Fig. 2. Remarkably, it is possible to find a temperature ($T_f = 0.8 < T_g$) where the force distributions, when scaled by the average force $\langle F \rangle$, are nearly identical for LJR12, LJR24, and experiments on static granular packings [5] over the entire range of forces. This implies that for sufficiently hard repulsive potentials, the shape of the distribution is not sensitive to the shape of the potential. In the limit of hard spheres, where the power of the repulsive term in the potential diverges, we expect similar behavior. In systems with softer potentials, such as Hertzian or harmonic repulsive springs, we also find the same shape of $P(F)$ as in Fig. 2 over nearly the entire range of forces at very low temperatures near the close-packing density [18]. These results suggest that the slight peak or plateau at small forces and exponential tail at large forces are generic features of $P(F)$ in athermal, experimental systems near the onset of jamming.

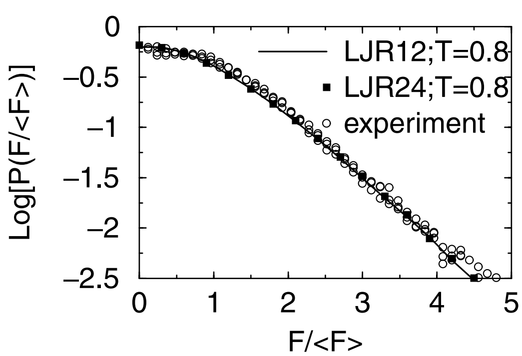

FIG. 2. $P(F/\langle F \rangle)$ versus $F/\langle F \rangle$ for both LJR12 and LJR24 after a quench to $T_f = 0.8$ (below T_g). Data from experiments on static granular packings from [5] are also shown. Note that all three sets of data have a plateau at small F and decay exponentially at large F.

Is a peak or plateau in $P(F)$ also observed in other jammed systems? To answer this, we have studied model two-dimensional foams [19,20], where bubbles are treated as circles that can overlap and interact via two types of pairwise interactions. The first is a harmonic repulsion that is nonzero when the distance between centers of two bubbles is less than the sum of their radii. The other is a simple dynamical friction proportional to the relative velocities of two neighboring bubbles. In foam, thermal motion of bubbles is negligible. We simulate a 400-bubble system at constant area with periodic boundary conditions in the x direction and fixed boundaries in the y direction. Bubble radii R_i are chosen from a flat distribution with $0.2 < R_i/\langle R \rangle < 1.8$.

At packing fractions ϕ above random close packing ($\phi_0 \approx 0.84$), quiescent foam is an amorphous solid with a yield stress σ_y. However, when shear stress $\sigma_{xy} > \sigma_y$ is applied, the foam flows. There are therefore two ways to approach the amorphous solid. We can either increase ϕ towards ϕ_0 at $\sigma_{xy} = 0$ (route 1), or we can decrease σ_{xy} towards σ_y at fixed $\phi > \phi_0$ (route 2). In Fig. 3, we show $P(F/\langle F \rangle)$ (only including harmonic elastic forces) along these two routes. The distributions along route 1 in the top frame were measured after quenching 50 configurations from $\phi_i \ll \phi_0$ to ϕ by increasing each particle radius. When $\phi < \phi_0$, $P(F/\langle F \rangle)$ increases monotonically as $F/\langle F \rangle$ decreases. As ϕ increases above ϕ_0, a local maximum forms near $\langle F \rangle$. A similar trend is found along route 2. To obtain these distributions, we averaged over at least 500 configurations with each brought to steady state for a strain of $\approx$10. In all cases shown, σ_{xy} exceeds σ_y, so the systems are flowing. We find that at large σ_{xy}, $P(F/\langle F \rangle)$ is nearly constant at small F. When σ_{xy} is lowered towards $\sigma_y \approx 0.10$, a peak in $P(F/\langle F \rangle)$ forms near

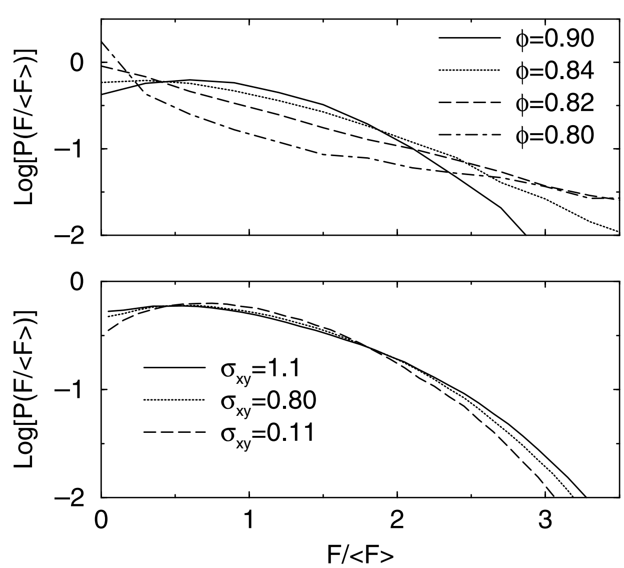

FIG. 3. Top: $P(F/\langle F \rangle)$ versus $F/\langle F \rangle$ for foams with $\sigma_{xy} = 0$ for several ϕ near random close packing. Bottom: $P(F/\langle F \rangle)$ for foams with $\phi = 0.9 > \phi_0$ and σ_{xy} lowered towards σ_y.

$F/\langle F\rangle \sim 1$. Similar behavior is observed in $P(F/\langle F\rangle)$ as a function of ϕ in experiments on sheared deformable disks [21] and as a function of confining stress in simulations of deformable spheres [10].

In this Letter, we have shown a connection between development of a yield stress, either by a glass transition or conventional jamming transition, and the appearance of a peak in $P(F)$. We have established that four different model supercooled liquids develop first a plateau and then a peak in $P(F)$ as temperature is lowered below the glass transition. We have also found (but not shown here) that the LJR12 liquid displays identical results for $P(F)$ as shear stress is lowered from the flowing state or as density is raised from the liquid state at fixed temperature [18]. For monodisperse liquids, we find that the appearance of a peak in $P(F)$ is well correlated with the onset of crystallization except at low densities where the yield stress is small [18]. The athermal foam likewise develops a peak in $P(F)$ as it approaches jamming along two different routes. Static granular packings exhibit a plateau or small peak in $P(F)$ as well. Thus, a peak in $P(F)$ appears as a wide variety of systems jam along each of the axes of the jamming phase diagram [4]. This suggests that jamming leads to common behavior and that the glass transition may resemble more conventional jamming transitions.

This still leaves the question of why formation of a peak or plateau in $P(F)$ appears to signal the development of a yield stress. The presence of the peak or plateau implies that there are a large number of forces near the average value. This is consistent with the existence of force chains, since each particle within a force chain must have roughly balanced forces on either side. We speculate that systems jam when there are enough particles in a force chain network to support the stress over the time scale of the measurement. Forces at the peak of $P(F)$ are among the slowest to relax: these forces correspond to separations near the first peak of $g(r)$, which stem from wave vectors near the first peak in the static structure factor, which are among the most slowly relaxing modes [22]. This implies that force chains observed in granular packings may also be important to the glass transition. The fact that force chains do not couple strongly to density fluctuations may explain why they have not been observed directly. However, large kinetic heterogeneities that appear near T_g [23] may be linked to the formation of force chains. This interpretation suggests that force chains may provide the key to the elusive order parameter for the glass transition.

We thank Susan Coppersmith, Heinrich Jaeger, Robert Leheny, Daniel Mueth, Thomas Witten, Walter Kob, and Gilles Tarjus for instructive discussions. Support from NSF Grants No. DMR-9722646 (C. S. O., S. R. N.), No. CHE-9624090 (C. S. O., A. J. L.), and No. PHY-9407194 (S. A. L., A. J. L., S. R. N.) is gratefully acknowledged.

[1] H. M. Jaeger, S. R. Nagel, and R. P. Behringer, Rev. Mod. Phys. **68**, 1259 (1996).
[2] D. J. Durian and D. A. Weitz, in *Kirk-Othmer Encyclopedia of Chemical Technology,* edited by J. I. Kroschwitz (Wiley, New York, 1994), 4 ed., Vol. 11, p. 783.
[3] M. D. Ediger, C. A. Angell, and S. R. Nagel, J. Phys. Chem. **100**, 13 200 (1996).
[4] A. J. Liu and S. R. Nagel, Nature (London) **396**, 21 (1998).
[5] D. M. Mueth, H. M. Jaeger, and S. R. Nagel, Phys. Rev. E **57**, 3164 (1998); D. L. Blair, N. W. Mueggenburg, A. H. Marshall, H. M. Jaeger, and S. R. Nagel (unpublished).
[6] P. Dantu, Géotechnique **18**, 50 (1968).
[7] C.-h. Liu, S. R. Nagel, D. A. Schecter, S. N. Coppersmith, S. Majumdar, O. Narayan, and T. A. Witten, Science **269**, 513 (1995); S. N. Coppersmith, C.-h. Liu, S. Majumdar, O. Narayan, and T. A. Witten, Phys. Rev. E **53**, 4673 (1996).
[8] G. Løvoll, K. J. Måløy, and E. G. Flekkøy, Phys. Rev. E **60**, 5872 (1999).
[9] F. Radjai, M. Jean, J.-J. Moreau, and S. Roux, Phys. Rev. Lett. **77**, 274 (1996); S. Luding, Phys. Rev. E **55**, 4720 (1997); A. V. Tkachenko and T. A. Witten, Phys. Rev. E **60**, 687 (1999).
[10] H. A. Makse, D. L. Johnson, and L. M. Schwartz, Phys. Rev. Lett. **84**, 4160 (2000); C. Thornton, KONA Powder Part. **15**, 81 (1997).
[11] S. Alexander, Phys. Rep. **296**, 65 (1998); T. Kustanovich, S. Alexander, and Z. Olami, Physica (Amsterdam) **266A**, 434 (1999); T. Kustanovich and Z. Olami, Phys. Rev. B **61**, 4813 (2000).
[12] D. N. Perera and P. Harrowell, Phys. Rev. E **59**, 5721 (1999).
[13] B. Widom, J. Phys. Chem. **86**, 869 (1982); L. L. Lee, D. Ghonasgi, and E. Lomba, J. Chem. Phys. **104**, 8058 (1996).
[14] M. P. Allen and D. J. Tildesley, *Computer Simulations of Liquids* (Oxford University Press, Oxford, 1987).
[15] W. Kob and H. C. Andersen, Phys. Rev. E **52**, 4134 (1995).
[16] C. Eloy and E. Clement, J. Phys. I (France) **7**, 1541 (1997); J. E. S. Socolar, Phys. Rev. E **57**, 3204 (1998); P. Claudin, J.-P. Bouchaud, M. E. Cates, and J.-P. Wittmer, Phys. Rev. E **57**, 4441 (1998); M. L. Nguyen and S. N. Coppersmith, Phys. Rev. E **59**, 5870 (1999).
[17] J. G. Powles and R. F. Fowler, Mol. Phys. **62**, 1079 (1987).
[18] C. S. O'Hern, S. A. Langer, A. J. Liu, and S. R. Nagel, (unpublished).
[19] D. J. Durian, Phys. Rev. Lett. **75**, 4780 (1995); Phys. Rev. E **55**, 1739 (1997).
[20] S. A. Langer and A. J. Liu, Europhys. Lett. **49**, 68 (2000); S. Tewari, D. Schiemann, D. J. Durian, C. M. Knobler, S. A. Langer, and A. J. Liu, Phys. Rev. E **60**, 4385 (1999).
[21] D. Howell, R. P. Behringer, and C. Veje, Phys. Rev. Lett. **82**, 5241 (1999).
[22] P.-G. de Gennes, Physica (Utrecht) **25**, 825 (1959). For applications to simulations of glass-forming liquids, see [15].
[23] M. D. Ediger, Annu. Rev. Phys. Chem. (to be published).